Optimized Generation of Functional Neutrophils and Macrophages from Patient-Specific Induced Pluripotent Stem Cells: Ex Vivo Models of X(0)-Linked, AR22(0)- and AR47(0)- Chronic Granulomatous Diseases

Brault, Julien; Goutagny, Erwan; Telugu, Narasimha; Shao, Kaifeng; Baquie, Mathurin; Satre, Véronique; Coutton, Charles; Grunwald, Didier; Brion, Jean-Paul; Barlogis, Vincent; Stephan, Jean-Louis; Plantaz, Dominique; Hescheler, Jürgen; Krause, Karl-Heinz [**and 2 more**]

How to cite

BRAULT, Julien et al. Optimized Generation of Functional Neutrophils and Macrophages from Patient-Specific Induced Pluripotent Stem Cells: Ex Vivo Models of X(0)-Linked, AR22(0)- and AR47(0)- Chronic Granulomatous Diseases. In: BioResearch open access, 2014, vol. 3, n° 6, p. 311–326. doi: 10.1089/biores.2014.0045

This publication URL: https://archive-ouverte.unige.ch/unige:82438

Publication DOI: 10.1089/biores.2014.0045

BioResearch Open Access
Volume 3, Number 6, December 2014

DOI: 10.1089/biores.2014.0045

Optimized Generation of Functional Neutrophils and Macrophages from Patient-Specific Induced Pluripotent Stem Cells: *Ex Vivo* Models of X^0-Linked, $AR22^0$- and $AR47^0$- Chronic Granulomatous Diseases

Julie Brault,[1,2] Erwan Goutagny,[1,2] Narasimha Telugu,[3] Kaifeng Shao,[3] Mathurin Baquié,[4] Véronique Satre,[5] Charles Coutton,[5] Didier Grunwald,[6] Jean-Paul Brion,[7] Vincent Barlogis,[8] Jean-Louis Stephan,[9] Dominique Plantaz,[10] Jürgen Hescheler,[3] Karl-Heinz Krause,[4] Tomo Šarić,[3] and Marie José Stasia[1,2]

Abstract

Chronic granulomatous disease (CGD) is an inherited orphan disorder caused by mutations in one of the five genes encoding reduced nicotinamide-adenine-dinucleotide-phosphate oxidase subunits, which subsequently lead to impairment in the production of microbicidal reactive oxygen species (ROS). In order to offer several cell line models of CGD and therefore support research on pathophysiology and new therapeutic approaches, we optimized protocols to differentiate induced pluripotent stem cells (iPSCs) from wild-type, X^0-, $AR22^0$- and $AR47^0$-CGD patient's fibroblasts into neutrophils and into macrophages. Aberrant genetic clones were discarded after chromosome karyotyping and array-comparative genomic hybridization analysis. All remaining iPSC lines showed human embryonic stem cell–like morphology, expressed all tested pluripotency markers and formed embryoid bodies that contained cells originating from all three primary germ layers. Furthermore, each CGD patient-specific iPSC line retained the $gp91^{phox}$, $p47^{phox}$, and $p22^{phox}$ mutations found in the corresponding patient's neutrophils. The average production of $CD34^+$ progenitors was of 1.5×10^6 cells after 10 days of differentiation of 10×10^6 iPSCs. They were terminally differentiated into about 3×10^5 neutrophils or into 3×10^7 macrophages. Based on morphological, phenotypical, and functional criteria both phagocyte types were mature and indistinguishable from the native human neutrophils and macrophages. However, neutrophils and macrophages derived from X^0-, $AR22^0$-, and $AR47^0$-CGD patient-specific iPSC lines lacked ROS production and the corresponding mutated proteins. To simplify the phagocytes' production upon request, progenitors can be cryopreserved. In conclusion, we describe a reproducible, simple, and efficient way to generate neutrophils and macrophages from iPSCs and provide a new cellular model for the $AR22^0$-CGD genetic form that has not been described before.

Key words: induced pluripotent stem cells; chronic granulomatous disease; NADPH oxidase; reactive oxygen species; neutrophils; macrophages; disease model; NOX2; $p47^{phox}$; $p22^{phox}$

[1]Techniques de l' Ingénierie Médicale et de la Complexité-Informatique, Mathématiques et Applications, Grenoble (TIMC-IMAG), Université Grenoble Alpes, Grenoble, France.
[2]Centre Diagnostic et Recherche sur la CGD (CDiReC), Pôle Biologie, [5]Laboratoire de Génétique Chromosomique, Pôle Couple/Enfant, [7]Service d'Infectiologie, Pôle Médecine Aigue et Communautaire, [10]Département de Pédiatrie, Pôle Couple/Enfants; Centre Hospitalier Universitaire de Grenoble, Grenoble, France.
[3]Center for Physiology and Pathology, Institute for Neurophysiology, Medical Faculty, University of Koln, Koln, Germany.
[4]Department of Genetic and Laboratory Medicine, Department of Pathology and Immunology, Geneva University Hospital and Medical School, Geneva, Switzerland.
[6]Institut de Recherches en Sciences et Technologies pour le Vivant/Commissariat à l'Energie Atomique, Grenoble, France.
[8]Service de Pédiatrie et Hématologie Pédiatrique, Assistance Publique-Hôpitaux de Marseille (AP-HM) – Hôpital de La Timone, Marseille, France.
[9]Service de Pédiatrie, Centre Hospitalier Universitaire de Saint-Etienne, Hôpital Nord, Saint-Etienne, France.

Introduction

In 2006 the Yamanaka's research group made a breakthrough discovery that added another dimension to the stem cell field.[1] They found that the introduction of four transcription factors (*Oct4*, *Sox2*, *Klf4*, and *cMyc*) into murine fibroblasts using retrovirus forces them to acquire embryonic stem cell (ESC)-like properties, such as self-renewal and pluripotency. These cells, named induced pluripotent stem cells (iPSCs), were shown to be morphologically, molecularly, and functionally similar to ESCs. The next year, two groups generated the first iPSCs from human fibroblasts.[2,3] Since then many types of somatic cells have been reprogrammed, including those from patients with different inherited disease types.[4] In addition, reprogramming methods became more efficient, reproducible and enable generation of transgene-free iPSCs under xeno-free conditions, which is an important prerequisite for their potential clinical application.[5] iPSCs can be differentiated into cells derived from the three embryonic germ layers (i.e., ectoderm, endoderm, and mesoderm) allowing the possibility to model diseases. iPSC-based disease models that closely recapitulate disease-specific phenotypes *in vitro* at the molecular and functional level were described for diverse inherited cardiovascular,[6] hematopoietic,[7] neurological,[8] and metabolic diseases,[9] most of which were monogenic. These patient-specific iPSC-based disease models have a great potential for investigation of disease pathophysiology *in vitro*, screening of new therapies or cell therapy applications with gene corrected cells.[10]

Chronic granulomatous disease (CGD) is a rare inherited immunodeficiency syndrome with an estimated prevalence of 1:250,000 in Europe.[11] CGD is characterized by recurrent and life-threatening infections in early childhood and is caused by mutations in one of the five genes encoding the proteins of the reduced nicotinamide-adenine-dinucleotide-phosphate (NADPH) oxidase complex expressed in phagocytic cells (neutrophils, monocytes/macrophages) and responsible for the production of antimicrobial and antifungal reactive oxygen species (ROS). The two transmembrane subunits, gp91^{phox} (NOX2) and p22^{phox}, and the cytosolic components p40^{phox}, p47^{phox}, and p67^{phox} are encoded by the *CYBB*, *CYBA*, *NCF4*, *NCF2*, and *NCF1* genes, respectively. The X-linked gp91^{phox} and the autosomal recessive p47^{phox} deficiencies represent the most common genetic forms of CGD (70% and 25%, respectively).[12–14] The main treatment is based on antibiotic and antifungal prophylaxis. At present, bone marrow transplantation is the only curative treatment proposed to the patients in case of a human leukocyte antigen-matched donor in the relatives. Gene therapy is still in development with variable results.[15,16] However, reliable cellular models of different genetic forms of CGD that could be used to develop new therapeutic approaches or study the pathophysiology of this disorder are missing. The only cell-based model mimicking the X-CGD are the knockout PLB-985 cells for the *CYBB* gene encoding gp91^{phox}. These cells can be differentiated into phagocytes.[17]

The feasibility to generate phagocytic cells from normal human iPSCs was first demonstrated by Slukvin's group in 2009.[18] After description of iPSCs derived from X-CGD mouse fibroblasts[19] Zou et al. reported in 2011 for the first time the generation of human X$^{\mathbf{0}}$-CGD neutrophils from iPSCs derived from human mesenchymal stromal cells.[20] They succeeded to rescue the oxidase-deficiency phenotype of CGD iPSC-derived neutrophils with a zinc finger nuclease-mediated safe harbor targeting approach. One year later, AR47$^{\mathbf{0}}$- and two X-CGD mature monocytes/macrophages were produced from iPSCs and shown to be similar to blood-derived cells from CGD patients.[21] Both obtained their phagocytic cells by hematopoietic differentiation of embryoid bodies (EBs) generated from iPSCs.[20,21] Hematopoietic differentiation of iPSCs can be induced directly from EBs or from coculture with stromal cells, such as OP9 cells.[18] Then production of mature macrophages was achieved in a feeder-free system,[21] while mouse and human neutrophils were generated in coculture with OP9 cells.[19,20]

The objectives of this study were (1) to elaborate a simple and unique protocol for the induction of hematopoiesis in order to generate unlimited quantities of neutrophils or macrophages from CGD patient-specific iPSCs, with the same genotypic and phenotypic characteristics as the original phagocytic cells of the patient; and (2) to model three genetic forms of CGD including X^0-linked, AR47$^{\mathbf{0}}$-CGD, and for the first time, the p22^{phox}-deficient form of CGD (AR22$^{\mathbf{0}}$-CGD). iPSC lines described in this study will allow for pathophysiological studies of these three CGD genetic forms by using mature CGD neutrophils or macrophages *ex vivo*, the screening of candidate drugs, and the development of new therapeutic approaches.

Materials and Methods

Ethics statement

Skin biopsies from X^0-linked, AR22^0-, and AR47^0-CGD patients were obtained after informed consent [Ethical permission Ref Comité de Protection des Personnes Sud-Est V (CPP): 09-CHUG-36, Ref Etude: FibroCGD, N° AFSSAPS: 2009-A00944-53].

Generation of human iPSCs and culture

Human dermal fibroblasts (hDFs) were isolated from the skin biopsy of CGD patients and cultured in fibroblast culture medium [Dulbecco's modified Eagle medium (DMEM)-glutamax supplemented with 10% fetal bovine serum (FBS), 1% nonessential amino acids (NEAA), 100 U/mL penicillin, 100 μg/mL streptomycin and 100 μM ß-mercaptoethanol (β-ME)]. All cell culture reagents mentioned in this chapter were purchased from Invitrogen, if not stated otherwise. Reprogramming of AR22^0- and AR47^0-CGD hDFs was performed using episomal vectors as previously described[22,23] with minor modifications.

Briefly, 1×10^6 hDFs were transfected with 2.5 μg of each of following episomal vectors: pCXLE-hOct3/4-shp53, pCXLE-hSox2-hKlf4, pCXLE-hLin28-hL-Myc (Addgene plasmid IDs: 27077, 27078, 27080, respectively) using Neon™ Transfection Device and a 100 μL Neon Tip according to the manufacturer's instructions (Invitrogen). X^0-CGD and wild-type (WT) iPSC lines were generated from the hDFs infected in a single experiment with equal amount of pMX-based retroviruses (Addgene) encoding the human transcription factors Oct3/4, Sox2, Klf4, and cMyc as described previously.[24] The iPSCs were maintained in an undifferentiated state on irradiated mouse embryonic fibroblasts (MEFs) in gelatin-coated wells with 1:1 DMEM: nutrient mixture F-12 (DMEM/F-12,) supplemented with 20% KnockOut™ Serum Replacement (KOSR), 8 ng/mL basic fibroblast growth factor (Miltenyi Biotec), 1%

NEAA, 2 mM L-glutamine and 100 μM β-ME (Sigma-Aldrich), at 37°C in normoxic conditions and 5% CO_2. The iPSCs were passaged using 1 mg/mL collagenase-IV treatment onto new MEFs. MEFs were cultured in DMEM high glucose with 20% heat-inactivated (FBS), 1% NEAA, and 1% penicillin-streptomycin.

Formation of embryoid bodies

To induce the formation of EBs, undifferentiated iPSC colonies were harvested by treatment with collagenase-IV and dispersed by scraping to maintain the cells in small clumps. Then these clumps were transferred in a 10-cm Petri dish and cultured in static suspension in DMEM/F-12 supplemented with 20% KOSR, 1% NEAA, 2 mM L-glutamine and 100 μM β-ME. The medium was changed every 3 days. After 21 days, EBs were plated and culture was continued for 14 days.

Induction of hematopoietic differentiation

The mouse bone marrow stromal cell line OP9 (ATCC® CRL-2749™) was maintained on gelatinized flasks in α-minimum essential medium (MEM) medium (Invitrogen) containing 20% non-heat-inactivated defined FBS Hyclone (ThermoFischer) and cells were plated at a density of 8×10^3 cells/cm^2. Hematopoietic induction was performed as previously described with slight modifications.[25] Briefly, 4 days after plating OP9 cells, iPSC colonies were harvested using 1 mg/mL collagenase-IV and small clumps were transferred onto OP9 cells. The differentiation culture medium consisted of α-MEM supplemented with 10% FBS Hyclone (ThermoFisher), 100 μM monothioglycerol (MTG) (Sigma-Aldrich), and 50 μg/mL ascorbic acid. The half medium of iPSCs/OP9 cocultures was changed on days 4, 6, 8, and 10. Cocultures were harvested at day 7, 10, or 13, and a single-cell suspension was prepared. Cells were washed with magnetic cell sorting (MACS) buffer (phosphate-buffered saline [PBS] with 5% FBS and 2 mM EDTA), filtered first through a 100-μm and then a 40-μm cell strainer (BD Biosciences) and used for flow cytometry, colony-forming cell assay, cell sorting, or further differentiations.

For some experiments, the single-cell suspension obtained from day 10 iPSCs/OP9 coculture was sorted after labelling with CD34 magnetic beads (Miltenyi Biotec) according to manufacturer's instructions. Viability and purity of the sorted CD34$^+$ cells was determined by flow cytometry. They were used for further analysis, hematopoietic differentiation or were frozen in Iscove's modified Dulbecco's medium (IMDM) supplemented with 20% FBS and 10% dimethylsulfoxyde (DMSO) (Sigma-Aldrich) and preserved in liquid nitrogen. Cryopreserved CD34$^+$ cells were thawed at 37°C and transferred in 1 mL of prewarmed IMDM, 20% FBS during 10 min and then 9 mL of medium were added to dilute the DMSO further. Cells were centrifuged and maintained in 10 mL of the same medium during 1 h at 37°C before further experiments.

Terminal differentiation into mature neutrophils

According to our protocol CD34$^+$ cells sorted from day 10 cocultures were maintained in suspension culture at a density of $3–5\times10^5$ cells/mL on poly-hydroxy-ethyl-methacrylate-coated (pHEMA, Sigma-Aldrich) 6-well plate for 4 days in IMDM supplemented with 20% FBS, 100 ng/mL stem cell factor, 100 ng/mL Flt3 ligand, 100 ng/mL interleukin (IL)-6, and 10 ng/mL thrombopoietin and 10 ng/mL IL-3. Then these cells were transferred onto fresh OP9 cells in six-well plates and the cytokines were replaced with 100 ng/mL granulocyte colony-stimulating factor alone for 11 days.[20,25] All the cytokines were provided from Miltenyi Biotec. Following differentiation, floating cells were collected for further analysis.

Terminal differentiation into mature macrophages

This protocol was adapted from published protocols.[21,25] Day 10 coculture-derived cells were cultured in suspension on pHEMA-coated T75 flasks in α-MEM containing 10% FBS Hyclone, 100 μM MTG, and 200 ng/mL granulocyte-macrophage colony-stimulating factor (GM-CSF) for 8 days, with half medium changed every 3 days. Then the medium was changed for IMDM with 10% FBS and 20 ng/mL macrophage colony-stimulating factor (M-CSF). All the cytokines were provided from Miltenyi Biotec. After 3 days, cells were filtered through a 40-μm cell strainer to eliminate aggregates and allowed to adhere onto 6- or 12-well plates in the same medium for 1 week, with half the medium changed after 3–4 days.

Colony forming unit assay

To determine the myeloid potential, CD34$^+$ sorted cells were plated in methylcellulose medium containing cytokines for myeloid differentiation (StemMACS HSC-CFU media 130-091-277, Miltenyi Biotec). Colony forming units (CFUs) were scored based on their morphology after 7–14 days of incubation.

May-Grunwald-Giemsa staining

Cells were washed in PBS, cytospun (Cytospin 4, ThermoScientific), and stained with May-Grunwald-Giemsa (MGG). Slides were examined using a microscope (Nikon Eclipse TS1000), and images were acquired with a Nikon DS camera.

Alkaline phosphatase staining

Alkaline phosphatase activity was detected as previously described.[24] Colonies were photographed using the phase-contrast microscope Zeiss.

Immunofluorescence staining

Cells were fixed in 4% paraformaldehyde (Sigma) for 10 min, blocked with PBS, 5% bovine serum albumin, 5% goat serum for 10 min and permeabilized (if needed) with 0.25% Triton X-100 (Sigma). iPSC colonies were stained with the following conjugated antibodies: anti-Oct3/4 PerCP-cyanine5.5, anti-Sox2 AlexaFluor647 (AF647), and anti–stage-specific embryonic antigen-4 (SSEA-4) fluorescein isothiocyanate (FITC) all purchased from BD Biosciences. EBs were stained with anti-CD31-coupled phycoerythrin (PE) (BD Biosciences) or with the following primary antibodies from the Human Embryonic Germ Layer Characterization Kit (SCR030; Merck Millipore): anti-Nestin, anti-α-smooth muscle actin (αSMA), anti-α-fetoprotein (αFP), anti-microtubule-associated protein 2 (MAP2), and anti-cardiac troponin I. Alexa fluor 488 (AF488)–conjugated anti-rabbit immunoglobin G (IgG) or anti-mouse IgG (Invitrogen) were used as secondary antibodies. Nuclei were stained with Hoechst 33258 1 μg/mL (Sigma). Images were acquired using either

a confocal laser-scanning microscope (TCS-SP2; Leica) or a fluorescence microscope (Olympus) and analyzed with ImageJ software.

Flow cytometry analysis

Cells were suspended in fluorescence-activated cell sorting (FACS) buffer (PBS, 2% FBS, 2 nM EDTA, 0.05% NaN_3) and stained with following conjugated antibodies all purchased from BD Biosciences excepted when stated otherwise: Vioblue®-conjugated anti-CD34 (Miltenyi Biotec); human leukocyte antigen-DR (HLA-DR) (Beckman Coulter), PE-conjugated anti-SSEA-3, Nanog, CD14, CD80 (Beckman Coulter), FITC-conjugated SSEA-4, CD11b, CD43, CD86 (Beckman Coulter), C-C chemokine receptor 7 (CCR7) (Beckman Coulter), allophycocyanin-conjugated anti-CD45, mannose receptor (MR) (Beckman Coulter), CD40 (Beckman Coulter), PerCP-cyanine5.5-conjugated Oct3/4, AF488-conjugated Tra-1-85 (Millipore), AF647-conjugated anti-Sox2, and Tra-1-81. Unconjugated antibody 7D5 directed against an external epitope of flavocytochrome b_{558} (D162-3; Clinisciences) and anti-$p22^{phox}$ (clone 44.1; Tebu Bio) with secondary antibody conjugated with AF633 (Invitrogen) and PE (Beckman Coulter), respectively, were used for analysis of NADPH oxidase subunit expression.[26,27] Control staining with appropriate isotype-matched control was included to establish thresholds for positive staining. Cell viability was determined by staining with 7-amino-actinomycin D (BD Biosciences). Cell fluorescence was quantified using a FACS Canto II (BD Biosciences). Data were collected and analyzed with the FACS DIVA software (BD Biosciences) and FlowJo software (Tree Star).

Myeloperoxidase activity in neutrophils

Myeloperoxidase staining was performed based on a previously published protocol.[28] Briefly, neutrophils were cytospun onto glass slides and were overlaid with a solution of benzidine (4,4′-diaminobiphenyl; Sigma-Aldrich) and sodium nitroprusside (Prolabo) for 3 min and then in the presence of H_2O_2 (Sigma-Aldrich) for 15 min. Slides were washed, dried, and stained with 20% Giemsa for 20 min. Images were acquired using a microscope Nikon Eclipse TS1000 equiped with a camera Nikon DS.

Transmission electron microscopy

Fixation of the membranes was performed by incubation in 2% glutaraldehyde in phosphate buffer for 1 h. The fixed tissue was washed three times with PBS, dehydrated in ethanol, embedded in epoxy resin, and processed for electron microscopy as described previously.[29] Sections were contrasted with uranyl acetate and lead citrate and observed with a Technai 20 electron microscope (FEI, www.fei.com).

Exocytosis experiment

IPSC–derived neutrophils were pretreated with 0.25 mg/mL cytochalasin B (CB) for 7 min at 37°C prior to stimulation with 5 μM f-Met-Leu-Phe (fMLF) (Sigma-Aldrich) for 15 min at 37°C to induce degranulation. Supernatants (S) and pellets (P) of resting and CB/fMLF-stimulated cells were assayed for lactoferrin and gelatinase (MMP9). The release of lactoferrin was measured by enzyme-linked immunosorbent assay (ELISA) kit using an anti-human lactoferrin antibody (Calbiochem No. 427275) according to the manufacturor's instruction. MMP9 release was determined by gelatin zymography, an electrophoretic method for measuring proteolytic activity as described previously.[30]

Cytokine profile assay

Macrophages were stimulated for 24 h with 1 ng/mL lipopolysaccharides (LPS) from *Pseudomonas aeruginosa* (Sigma-Aldrich). The detection of 12 inflammatory cytokines was performed on cell media using a Multi-Analyte Profiler ELISArray™ kit (MEM-004A, Sigma-Aldrich) according to the manufacturor's instructions.

Phagocytosis assay by flow cytometry

Macrophages were incubated with AF488 fluorescent head-killed particles of *Staphyloccocus aureus* (Invitrogen) or with Zymosan particles isolated from *Saccharomyces cerevisiae* labeled with AF488 (Invitrogen) at a multiplicity of infection of 5:1. After 30 min at 37°C, the reaction was stopped by placing cells on ice.[31] Cells were then analyzed by flow cytometry with a FACS Canto II (BD Biosciences), before and after adding 1 mg/mL trypan blue (Sigma Aldrich). Data were treated with FlowJo software (Tree Star).

Detection of reactive oxygen species produced by neutrophils or macrophages

Reactive oxygen species (ROS) production in phagocytic cells was measured by flow cytometry in presence of 0.5 μM dihydrorhodamine-1,2,3 (DHR) (Tebu Bio), by chemiluminescence in presence of luminol and horseradish peroxidase (HRPO) or by the nitro blue tetrazolium (NBT)-reduction test after opsonized latex beads phagocytosis as previously described.[32,33]

Karyotyping

Chromosome karyotyping (R-banding) was performed for each iPSC line using a protocol kindly provided by Dr. Pellestor (Laboratoire de Génétique Chromosomique, CHU de Montpellier, France). iPSCs were incubated with KaryoMAX® Colcemid™ (Invitrogen) at 0.1 μg/mL during 90 min at 37°C. Cells were harvested using TrypLE (Invitrogen) and washed with PBS-2% FBS. Hypotonic choc was obtained after 20 min incubation at 37°C with prewarmed 0.75 M KCl and then stopped by adding cold fixation solution (methanol/ acetic acid 3:1 v/v) and placing the cells on ice for 4 min. Then, cells were fixed by repeating three cycles of mixing with the cold fixation solution followed by centrifugation. Cells were finally incubated for 1 h at −20°C, centrifuged, suspended in fixation solution, and stored at −20°C before analysis. A total of 20 metaphases were examined, five of them karyotyped using a microscope Zeiss and a MetaSystems Ikaros® karyotyping system.

Genomic DNA amplification and sequencing from iPSCs

To verify the genetic defects, exon sequences of the genes involved (*CYBA*, *CYBB*, and *NCF1*) were amplified by polymerase chain reaction using appropriates forward and backward primers[34] from genomic DNA purified from the iPSCs using a purification kit (FlexiGene DNA kit, Qiagen). They were then sequenced by Eurofins MWG Operon (Germany).

Array-comparative genomic hybridization

Array-comparative genomic hybridization (array-CGH) was performed using a 60,000-oligonucleotide microarray (Human Genome CGH Microarray Kit 60K, Agilent Technologies), following the manufacturer's instructions. The average spacing of the probes was 54 kb. DNA from the patient (or patient-derived iPSCs) was compared with a homemade reference DNA. Genomic Workbench software, standard edition 6.5 (Agilent) was used to interpret the results with the following parameters: aberration algorithm ADM-2, threshold 6.0, fuzzy zero, centralization, and moving average window 0.5–1 Mb. A copy number variation (CNV) was noted if at least three contiguous oligonucleotides showed an abnormal log2 ratio ($>+0.58$ or <-1 according to the cyanin 5 deviation). Coordinates of all variations or probes are based on the University of California Santa Cruz (UCSC) GRCh37/hg19 assembly.[35,36]

Statistical analysis

The nonparametric Wilcoxon signed rank test for paired samples was used to compare means for WT iPSC clones 3 and 4 and X^0-CGD iPSC clones 1 and 6 across the time of hematopoietic differentiation. A two-way mixed model repeated measures analysis of variance followed by Tukey's post-hoc test was used for each marker separately to determine differences between days 7, 10, and 13. The normality was tested by Shapiro-Wilk test and normal quantile plots, and the equality of variance was tested by the use of Levene test. Results are therefore expressed as mean ± standard error of the mean (SEM). Statistical differences were considered to be significant after Tukey adjustment if $p \leq 0.05$. Statistical analysis were performed using SAS 9.3 (SAS Institute Inc.). Graphical representations were done with GraphPad Prism 5 software with data presented as the mean ± SEM. The statistical significances of the differences were evaluated by Student's *t*-test.

Results

Production and characterization of WT, X^0-linked, $AR22^0$-, and $AR47^0$-CGD patient-specific iPSC lines

Two to three clones of each iPSC line were established from fibroblasts isolated from a healthy donor or three CGD patients suffering from different genetic types according to the procedures mentioned in ''Material and Methods.'' All the $AR22^0$-CGD iPSC colonies cultured in an undifferentiated state showed a specific hESC-like morphology, a high alkaline phosphatase activity, and the expression of pluripotency markers Oct4, Sox2, Nanog, SSEA-3, SSEA-4, and Tra-1-81 as determined by immunocytochemistry and/or flow cytometry (Fig. 1A). Furthermore, they formed EBs *in vitro* containing cells originating from the three germ layers (ectoderm, mesoderm, and endoderm) as shown by expression of lineage-specific markers (Fig. 1B). The same results were obtained from all the iPS cell lines (WT, X^0-CGD, and $AR47^0$-CGD) (data not shown). They also retained the *CYBB, CYBA*, and *NCF1* mutations found in the patient fibroblasts (Fig. 2A) and exhibited normal karyotype (Fig. 2B).

Further analysis by array-CGH was performed on every clone to detect whether major chromosomal abnormalities or CNV were induced following iPSC reprogramming. Two large telomeric deletions were found in the X^0-CGD iPS clone 7 that was excluded from further experiments (Fig. 2C). The first deletion is a 6.43-Mb loss extending from base pair 14,316 (first deleted oligonucleotide) to base pair 6,357,632 (last deleted oligonucleotide) (NCBI, hg 19) from the 18p telomere. The second is an 18.5-Mb deletion from base pair 59,481,918 (first deleted oligonucleotide) to 77,982,126 (last deleted oligonucleotide) from the 18p telomere. No other abnormalities were found in the other iPSC clones.

Induction of hematopoietic differentiation to generate $CD34^+$ progenitors

An efficient hematopoietic differentiation of iPSCs can be induced by coculture with OP9 bone marrow mouse stromal cells.[37,38] In order to optimize the timing for generation of $CD34^+$ progenitor cells from iPSCs, kinetics of differentiation of X^0-linked CGD and WT iPSC lines were analyzed by the disappearance of pluripotency markers and appearance of the hematopoietic marker CD34 using flow cytometry at day 7, 10, or 13 of coculture with OP9 cells (Fig. 3A). Expression of Tra-1-81 and SSEA-4 markers was markedly decreased at day 7, confirming the differentiated state of iPSCs at that time.

Undifferentiated iPSCs (day 0) did not express the hematopoietic markers CD34 (data not shown), but during the time course of OP9 coculture, the proportion of $CD34^+$ cells significantly peaked at day 10 of differentiation for both the WT and X^0-CGD iPSCs (Fig. 3A). Two different clones of the X^0-CGD and WT-iPSCs were used and no significant difference in the timing of differentiation was observed. These preliminary results showed that the optimal production of $CD34^+$ cells occurred at day 10 of coculture. Therefore, in all subsequent experiments, hematopoietic differentiation was terminated at that time. In order to ascertain their hematopoietic potential, $CD34^+$ progenitors obtained at day 10 were subjected to the colony-forming cells (CFC) assay. $CD34^+$ were sorted cells after labelling with CD34 magnetic beads and cultured in methylcellulose with hematopoietic cytokines. Under these conditions these cells gave rise to myeloid colonies with typical morphologies (CFU-granulocyte [CFU-G], CFU-macrophage [CFU-M], and CFU-GM), and MGG staining confirmed the identity of these colonies by the presence of mature neutrophils, macrophages or both cell types (Fig. 3B).

In order to save time for a rapid production of mature phagocytic cells upon request, we next tested the impact of freezing/thawing on $CD34^+$ progenitors' ability. CFC assay was performed after freezing and subsequently thawing of the $CD34^+$ progenitors and we demonstrated identical progenitor ability of the $CD34^+$ cells before and after thawing (Fig. 3C). Moreover, the majority (85%–90%) of these $CD34^+$ progenitors were $CD43^-$ $CD45^-$ (data not shown). Finally, the number of $CD34^+$ cells obtained using this protocol was analyzed for the WT and the three CGD iPSC lines (X^0-linked, $AR22^0$-CGD, and $AR47^0$-CGD). The average production of $CD34^+$ cells was of 3.3×10^5 cells from 2×10^6 iPSCs per 75 cm^2 flask ($s^2 = 1.1 \times 10^5$, range of $1.8–5.4 \times 10^5$ cells in 32 independent cultures) (Fig. 3D) with a purity of sorting cells about 87.4% ($s^2 = 7.2\%$, range of 62.6%–96.7% in 32 independent cultures) and a cell viability of 79.3% ± 5.0% as determined by trypan blue exclusion assay. These data confirmed that our selected protocol was able to generate

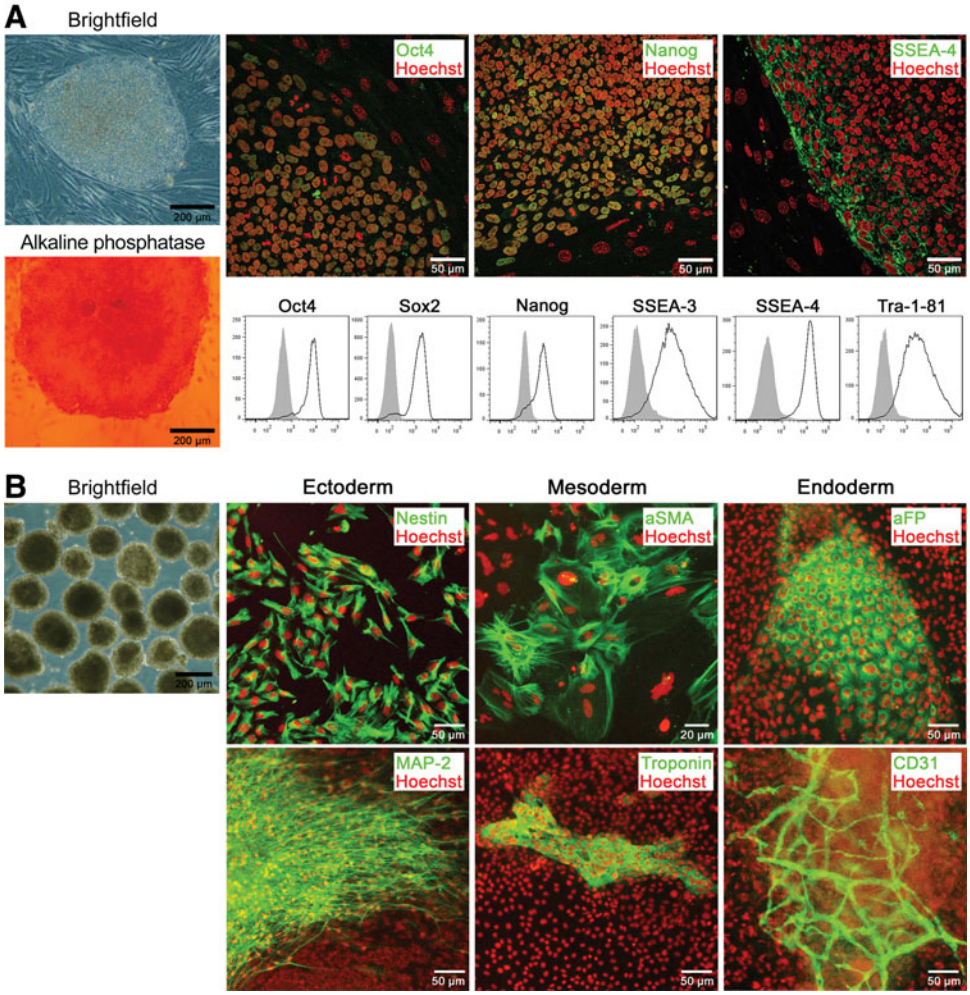

FIG. 1. *In vitro* characterization of induced pluripotent stem cells (iPSC) lines from AR22^0-CGD (chronic granulomatous disease) patients. **(A)** Representative image of human embryonic stem cell (ESC)-like morphology of iPSC line. A high alkaline phosphatase activity in iPSCs is shown by phase-contrast microscopy (scale bars: 200 μm). Immunofluorescence confocal images (*upper panel*) show the expression of pluripotency-associated transcription factors Oct4 and Nanog and the surface marker stage-specific embryonic antigen-4 (SSEA-4; in green) with nuclei counterstained with Hoechst in red (scale bars: 50 μm). Fluorescence-activated cell sorting analysis reveals the expression of the transcription factors Oct4, Sox2, and Nanog, and the surface markers SSEA-3, SSEA-4, and Tra-1-81. Isotype controls are represented by gray-filled curves. These results are representative of 3 independent experiments. **(B)** Characteristic morphology of embryoid bodies (EBs) was assessed by phase-contrast microscopy (scale bar: 200 μm). Immunofluorescence analysis of *in vitro* differentiated EBs demonstrates the expression of specific markers of the three embryonic germ layers: ectoderm (nestin and MAP2: green), mesoderm (αSMA and troponin: green) and endoderm (α-AFP: green; CD31: red). Nuclei were counterstained with Hoechst in red. Scale bars (20 μm or 50 μm) are shown on each panel.

a large number of CD34$^+$ cells with myeloid differentiation potential, which is conserved even after sorting and thawing.

Successful differentiation of CGD iPSCs into mature neutrophils

Fifteen days after initiating the differentiation of sorted CD34$^+$ cells into neutrophils using the protocol described in Fig. 4, floating cells were harvested and analyzed. Morphological analysis of AR22^0-CGD iPSC-derived neutrophils by MGG staining and electron microscopy revealed that they looked similar to blood-derived neutrophils: they were characterized by a poly-segmented nucleus and the presence of different types of more or less dense granules that suggests the development of diverse populations of granules during maturation (Fig. 5A). The average number of floating cells obtained from 1×10^6 CD34$^+$ cells was 1.68×10^5 cells (range: 0.55–2.7×10^5 cells in 16 independent cultures). We chose to show the AR22^0-CGD iPSC-derived neutrophils because this disease model has never been reported before. Similar data for maturation of neutrophils were also obtained from WT and other CGD-derived iPSC lines (data not shown). Based on their morphology after MGG staining, the purity of neutrophils was estimated to be around 50%–70% in neutrophil populations derived from all iPSC lines. Approximately 10% were monocytes/macrophages and 20%–40% were myeloid progenitor cells. The average yield of neutrophils was around 3×10^5 mature cells from 1.5×10^6 CD34$^+$ cells (range: 6.0×10^4 to 0 7.2×10^5 cells in 16 independent cultures). The proportion of myeloperoxidase (MPO)-positive

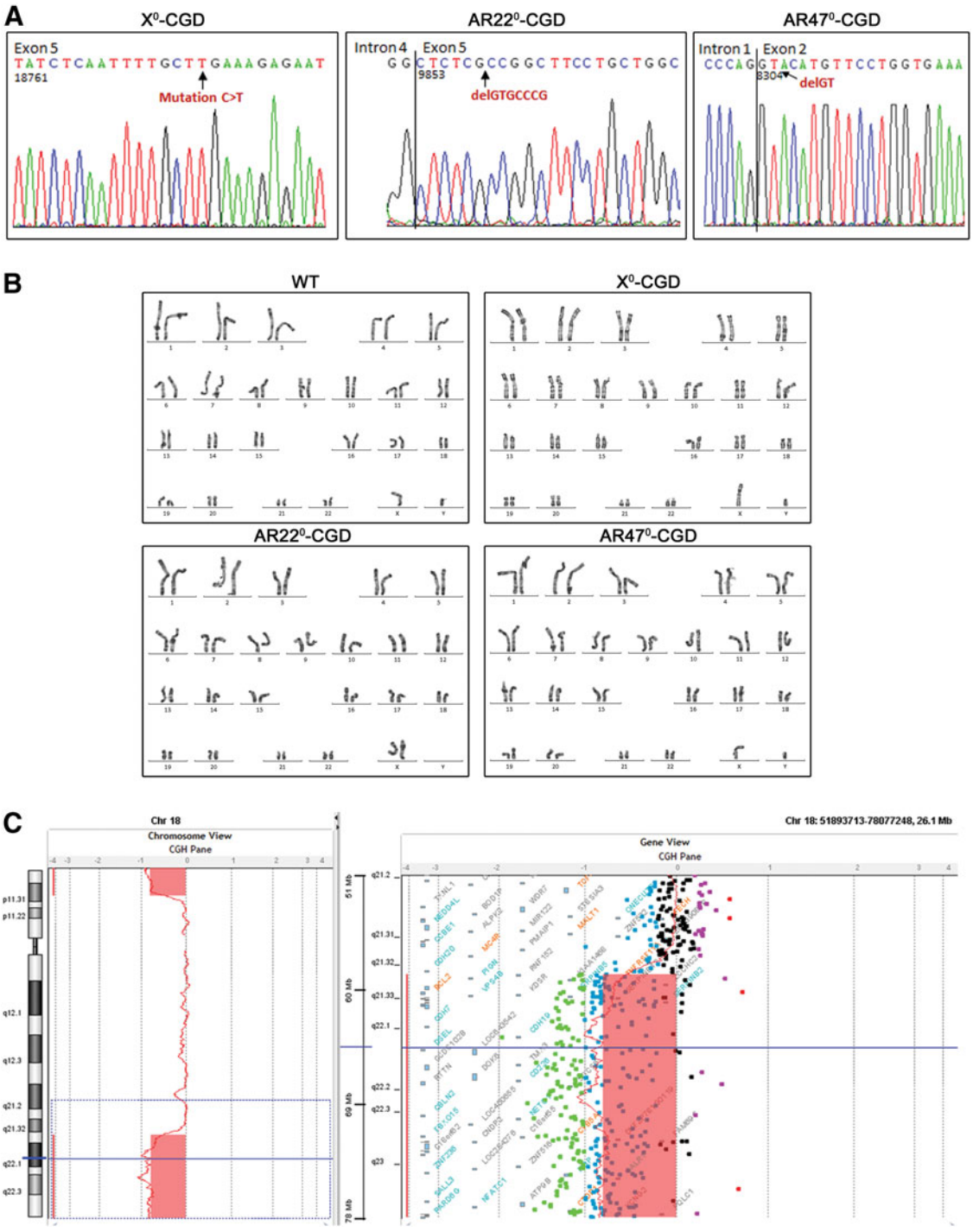

FIG. 2. Genetic characterization of iPSC lines from healthy and X^0-linked $AR22^0$- and $AR47^0$-CGD patients. **(A)** Sequencing analysis confirms that CGD-iPSC lines retain the mutations of CGD patients. X^0-linked CGD: c.469C > T nonsense mutation in exon 5 of *CYBB* gene leading to a stop codon TGA in the $gp91^{phox}$ protein (p.Arg157X); $AR22^0$-CGD: deletion of 7pb in exon 5 of *CYBA* gene (c295_301delGTGCCCG) leading to a premature stop codon in the $p22^{phox}$ protein (p.Val99-ProfsX90); $AR47^0$-CGD: GT dinucleotide deletion at the beginning of the exon 2 of the *NCF1* gene (c.75_76delGT) leading to a premature stop codon in the $p47^{phox}$ protein (p.Tyr26HisfsX26). **(B)** Karyotype analysis for wild-type (WT) and the three CGD-iPSC lines shows normal human karyotype (46XX or 46XY). **(C)** Array-comparative genomic hybridization (array-CGH) profile of chromosome 18 from X^0-CGD iPSC clone 7 shows two large telomeric deletions (6.43 Mb and 18.5 Mb).

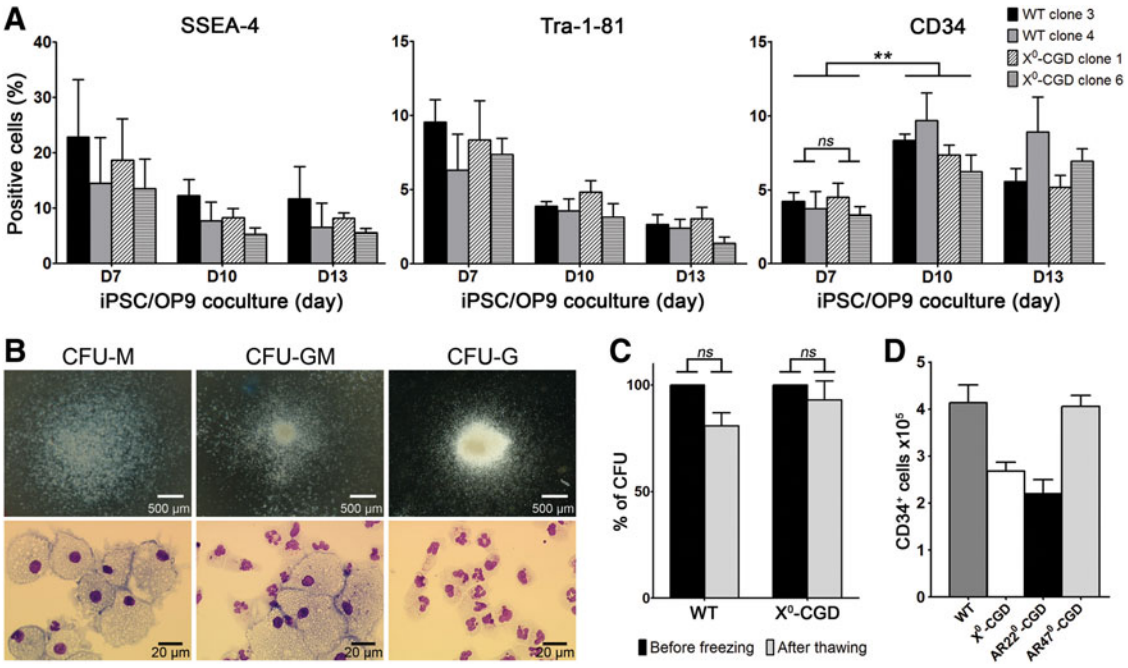

FIG. 3. Hematopoietic differentiation during WT and X^0-CGD iPSC/OP9 coculture and generation of iPSC-derived $CD34^+$ hematopoietic progenitors. **(A)** Kinetic analysis of the expression of pluripotency (SSEA-4 and Tra-1-81) and hematopoietic (CD34) markers during *in vitro* hematopoietic differentiation of iPSC/OP9 coculture (days 7, 10, and 13). Two clones for each iPS cell line were used. Data represent means ± SEMs of $n=3$ for SSEA-4 and Tra-1-81 and $n=4$ for CD34; $^{**}p<0.01$. **(B)** Hematopoietic potential of $CD34^+$ progenitors. Colony forming unit (CFU) assay performed on iPSC-derived $CD34^+$ cells isolated from iPSC/OP9 coculture at day 10 shows representative myeloid colonies (CFU-M, -GM, and -G) generated after 14 days of incubation (scale bars: 500 μm) and May-Grunwald-Giemsa (MGG) staining of isolated cells from these colonies (scale bars: 20 μm). **(C)** Effect of freezing/thawing of $CD34^+$ progenitors at day 10 on their hematopoietic differentiation potential. Results are expressed as percentage of CFU before freezing and after thawing of day 10 $CD34^+$ cells. $n=4$; *ns*: nonsignificant. **(D)** Average yield of $CD34^+$ cells sorted after 10 days of coculture of WT, X^0-linked, $AR22^0$-, and $AR47^0$-CGD iPSCs with OP9 cells ($n=8$). Data represent means ± SEMs.

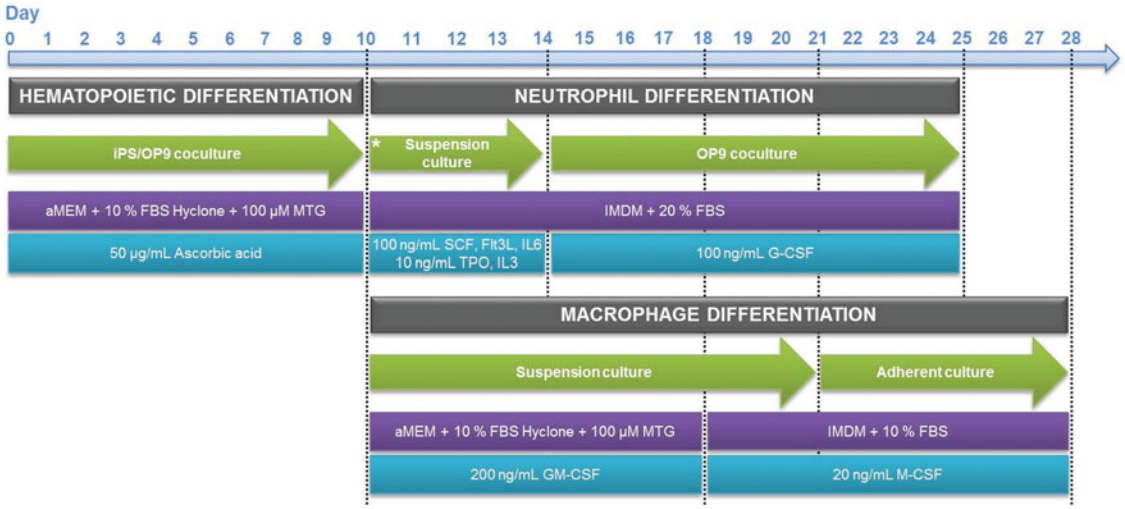

FIG. 4. Experimental design for the generation of mature neutrophils and macrophages from iPSCs. Schematic representation of the two-step protocol used to obtain $CD34^+$ hematopoietic progenitors (D10) and further differentiation into mature neutrophils (D25) and macrophages (D28). White star (*) indicates that $CD34^+$ progenitors were isolated from day-10 coculture by magnetic cell sorting. FBS, fetal bovine serum; G-CSF, granulocyte colony-stimulating factor; GM-CSF, granulocyte-macrophage colony-stimulating factor; IL, interleukin; IMDM, Iscove's modified Dulbecco's medium; M-CSF, macrophage colony-stimulating factor; MEM, minimal essential medium; MTG, monothioglycerol; SCF, stem cell factor; TPO, thrombopoietin.

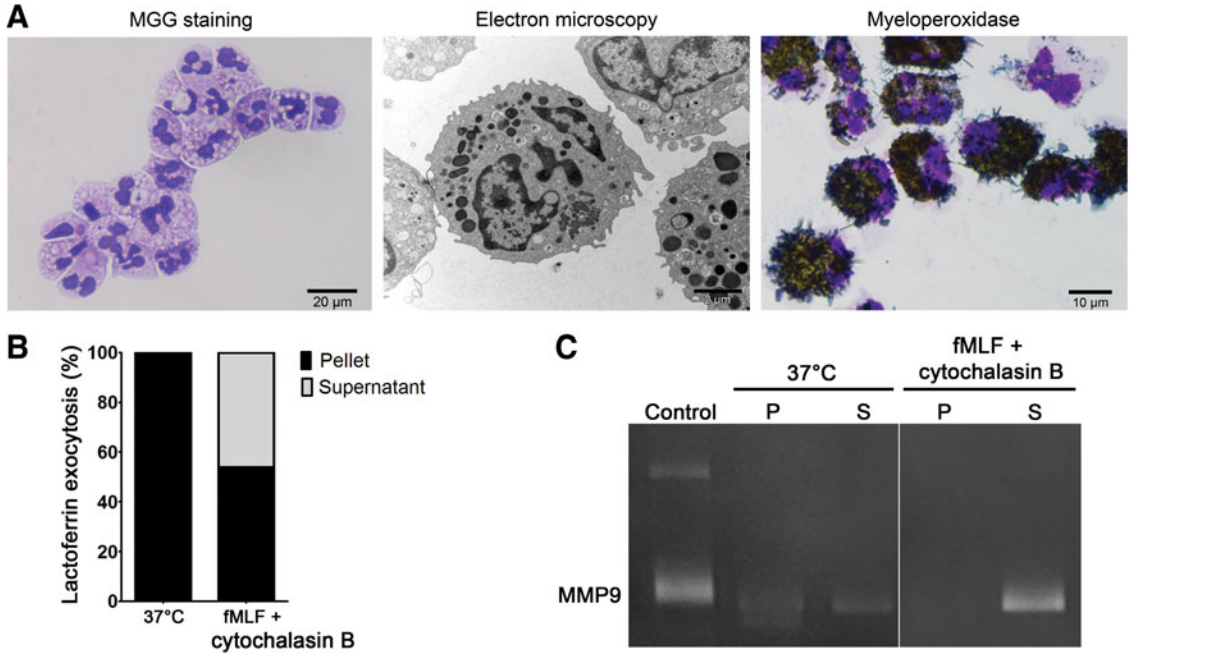

FIG. 5. Phenotypic characterization of AR22^0-CGD iPS-derived neutrophils. **(A)** Characteristic mature neutrophil morphology shown by MGG staining and electron transmission microscopy. Neutrophils have poly-segmented nuclei and different cytoplasmic granules (*left* and *middle panels*) and high myeloperoxidase activity revealed by enzymatic assay confirming the presence of primary granules (*right panel*). Scale bars (20 μm, 2 μm, and 10 μm) as shown on each panel. **(B)** Lactoferrin release from AR22^0-CGD iPSC-derived neutrophils treated with cytochalasin B and activated with f-Met-Leu-Phe (fMLF) as described in ''Material and Methods.'' Results are expressed as the percentage of lactoferrin present in the supernatant or in the pellet of unstimulated and fMLF-stimulated neutrophils and are representative of two independent experiments. **(C)** Gelatin zymography performed with the pellet (P) and the supernatant (S) of unstimulated and stimulated neutrophils. Areas of proteolytic activity appear as clear bands against a dark blue background where the gelatinase (MMP9) has digested the substrate. The gelatinolytic activity of purified MMP-9 as a control is shown on the first column. This result is representative of two independent experiments.

cells was scored and revealed that the AR22^0-CGD iPSC-derived neutrophils contained MPO, confirming the presence of azurophilic granules in these cells (Fig. 5A).

To further characterize the functional phenotype of iPSC-derived neutrophils, we determined the nature of different subtypes of granules by measuring lactoferrin exocytosis and matrix-metalloprotease 9 (MMP9) activity after inducing the degranulation of neutrophils by fMLF stimulation in the presence of cytochalasin B. Lactoferrin and matrix-metalloprotease 9 (MMP9), markers of specific and tertiary granules, respectively, were readily detected in iPSC-derived neutrophils (Fig. 5B, C). Similar results were obtained with the WT and the two other CGD iPSC-derived neutrophils confirming normal degranulation activity and enzymatic content in all these cell populations (data not shown).

Successful differentiation of CGD iPSCs into mature macrophages

After macrophage differentiation as described above (Fig. 4), adherent cells showed a fibroblastoid appearance and process extension, which are morphological characteristics of mature macrophages. Moreover, MGG staining and electron microscopy showed that these adherent cells obtained after 28 days of differentiation were morphologically mature macrophages with a round nucleus and large vacuoles in the cytoplasm (Fig. 6A). The average production of macrophages was around 3×10^7 mature cells from 10×10^6 iPS cells (range: 1.2–12.3$\times10^7$ cells in 12 independent cultures). Phenotypic analysis by flow cytometry confirmed that more than 90% of the adherent cells were CD11b$^+$ CD14$^+$ CD45$^+$ cells (Fig. 6B). To further analyze the subtype of AR22^0-CGD iPSC-derived macrophages, we measured by flow cytometry the expression of the human leucocyte antigen D-related (HLA-DR), the mannose receptor (MR, CD206), and the CC-chemokine receptor 7 (CCR7). This adherent population was predominantly positive for MR (80%–92%) and negative for both HLA-DR and CCR7 expression suggesting a M2c phenotype. Finally, we demonstrated that the AR22^0-CGD macrophages expressed the antigen presentation co-stimulatory molecules CD40, CD80, and CD86 (Fig. 6B). Similar expression levels of these molecules were detected in the WT and the other CGD iPSC lines (data not shown).

Analysis of the inflammatory response of macrophages derived from WT iPSCs and X^0-, AR47^0-, and AR22^0-CGD iPSC lines after LPS stimulation revealed that all these cells secrete IL-6, IL-8, and IL-10 into the medium supernatant while the rate of production of TNFα and GM-CSF was low and more dependent on the cell line (Fig. 6C). IL-8 was produced even in the unstimulated WT and CGD macrophages. After stimulation with either fluorescent bacteria (*S. aureus*) or yeast particles (opsonized zymosan from *Saccharomyces cerevisiae* [ZOPS]) all of the iPSC-derived macrophages demonstrated phagocytosis ability (Fig. 6D).

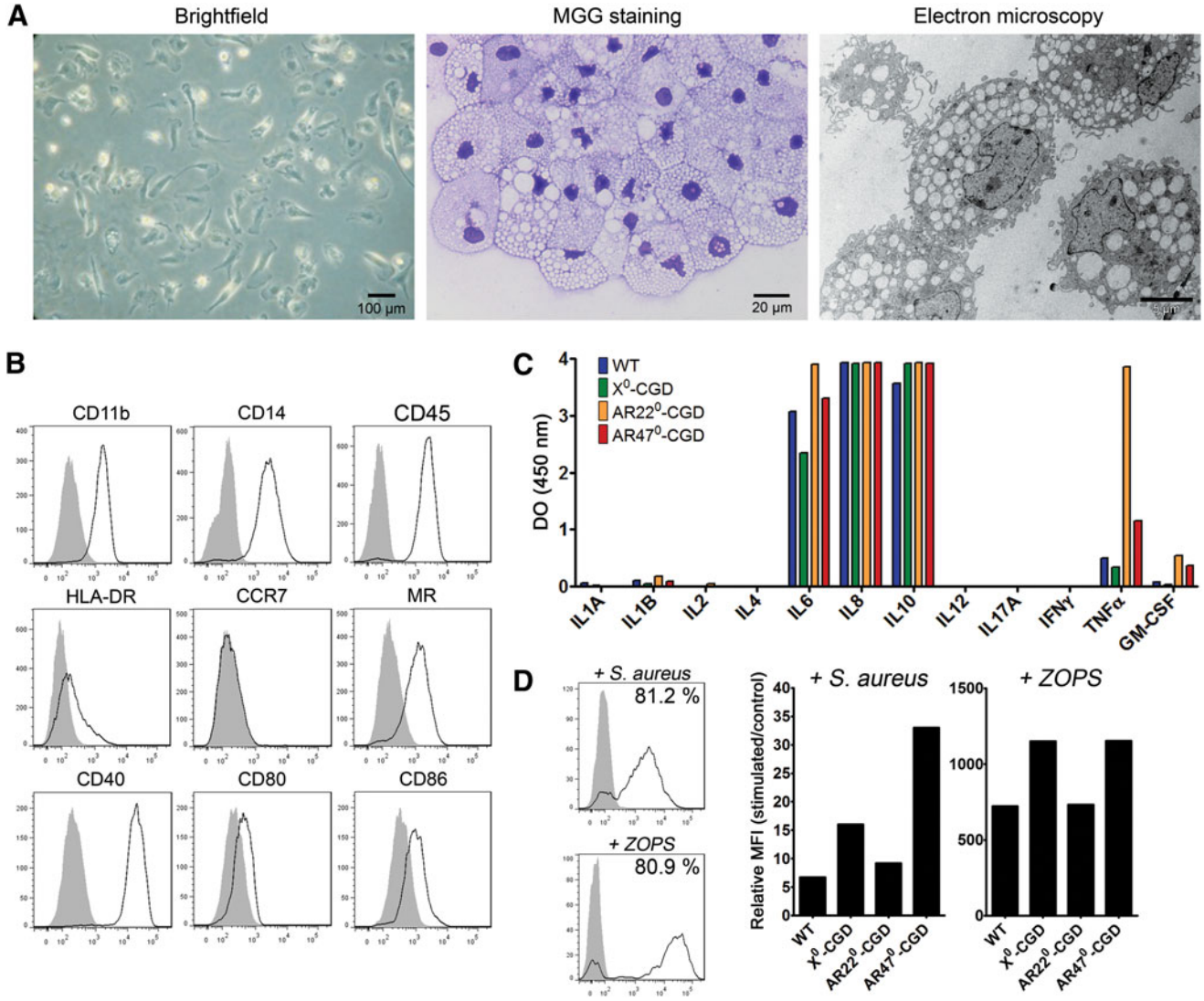

FIG. 6. Phenotypic characterization of iPSC-derived macrophages. **(A)** Morphology of adherent cells obtained after 28 days of differentiation, MGG staining, and electron transmission microscopy showing the characteristic morphology of $AR22^0$-CGD iPSC-derived macrophages with round nucleus and cytoplasmic vesicles. Scale bars (100 μm, 20 μm, and 5 μm) are shown in each panel. **(B)** Phenotypic analysis by flow cytometry of adherent $AR22^0$-CGD iPSC-derived macrophages stained with antibodies specific for CD11b, CD14, CD45, HLA-DR, CCR7, MR, CD40, CD80, and CD86 or isotype-matched controls (*gray* fill); these results are representative of two experiments. **(C)** Cytokine profiles of WT and CGD iPSC-derived macrophages activated for 24 hours with 1 ng/mL lipopolysaccharides (LPS). Measurement of cytokine production is performed in supernatant using a Multi-Analyte Profiler ELISArray^{TM} kit. **(D)** Phagocytosis experiments of fluorescent *Staphyloccocus aureus* or zymosan particles by WT and CGD iPSC-derived macrophages. Results are expressed as the mean fluorescence intensity ratio of stimulated and unstimulated macrophages (*right panels*) as determined after flow cytometry (*left panels*) and are representative of two experiments.

FIG. 7. Functional characterization of neutrophils and macrophages derived from WT and CGD-iPSCs. **(A)** Expression of the NADPH oxidase subunits $gp91^{phox}$ and $p22^{phox}$ in neutrophils and macrophages derived from WT and CGD-iPSC lines. Cells were incubated with the NOX2 monoclonal antibody 7D5 or the monoclonal antibody against $p22^{phox}$ (clone 44.1) respectively, and then with a phycoerythrin-conjugated anti-mouse immunoglobin G (IgG) (H + L). Mouse IgG1 isotype was used as an irrelevant monoclonal antibody. Results are representative of three independent experiments. **(B)** Nitro blue tetrazolium (NBT) reduction assay on opsonized latex beads-activated WT or CGD iPSC-derived neutrophils and macrophages ($n = 2$). Reactive oxygen species (ROS)-mediated NBT reduction is shown as blue formazan precipitates in WT neutrophils and macrophages only (scale bars: 20 μm). **(C)** Images of dihydrorhodamine-1,2,3 (DHR) dot plot showing ROS production by phorbol 12-myristate 13-acetate (PMA)-stimulated neutrophils derived from WT and $AR22^0$-CGD-iPSCs. **(D)** Kinetics of H_2O_2 production measured by luminol-enhanced chemiluminescence assay during 60 min after stimulation of WT and CGD neutrophils (*upper panels*) or macrophages (*lower panels*) with phorbol 12-myristate 13-acetate (PMA) or opsonized zymosan (ZOPS) particles. Inserts represent enlargement of the Relative Luminescence Unit Scale for neutrophils. Results are representative of three independent experiments.

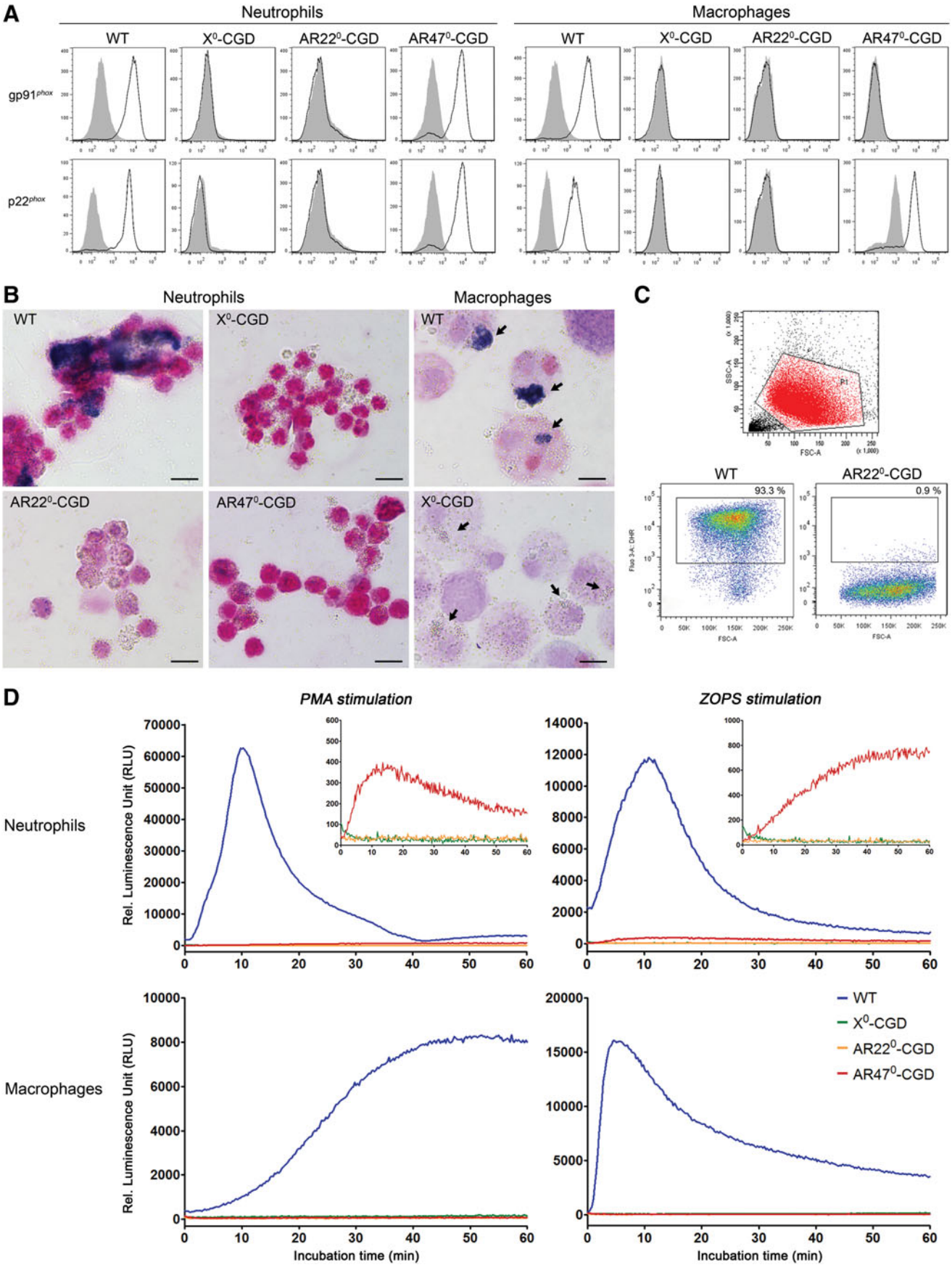
A
Neutrophils
Macrophages
WT
X⁰-CGD
AR22⁰-CGD
AR47⁰-CGD
gp91phox
p22phox
B
Neutrophils
Macrophages
C
P1
SSC-A
FSC-A
93.3 %
0.9 %
D
PMA stimulation
ZOPS stimulation
Neutrophils
Macrophages
Rel. Luminescence Unit (RLU)
Incubation time (min)
WT
X⁰-CGD
AR22⁰-CGD
AR47⁰-CGD

iPSC-derived neutrophils and macrophages as in vitro *models of three CGD forms*

Expression analysis of gp91^{phox} and p22^{phox}, the two transmembrane subunits of the NADPH oxidase complex, was performed by flow cytometry in WT and all the CGD phagocytes. Both subunits were absent in AR22^0-CGD and X^0-linked CGD neutrophils and macrophages but present in AR47^0-CGD neutrophils and macrophages (Fig. 7A). Then, the capacity of phagocytic cells to produce ROS after soluble or particulate stimuli activation of the NADPH oxidase was evaluated by different methods. The WT and CGD neutrophils and macrophages were able to phagocyte opsonized latex beads but the purple formazan from the NBT reduction was only visible in the WT iPSC-derived phagocytes (Fig. 7B). These results were confirmed in the DHR assay by the absence of ROS production in the phorbol 12-myristate 13-acetate (PMA)-stimulated CGD neutrophils (Fig. 7C) and by chemiluminescence in both neutrophils and macrophages upon PMA or ZOPS stimulation (Fig. 7D). WT phagocytic cells showed a high ROS production, but with distinct kinetics depending on the cell and the stimuli types.

First ROS production was rather similar in the WT neutrophils and macrophages for ZOPS stimulation. PMA induced a higher stimulation than ZOPS in the neutrophils whereas it was the contrary in the macrophages. In addition, there was a striking difference in the kinetics of ROS production after ZOPS stimulation between neutrophils and macrophages, with macrophages exhibiting more prolonged ROS production after yeast phagocytosis than neutrophils. Finally, a weak ROS production was detected in AR47^0-CGD neutrophils compared with the other types of CGD neutrophils after PMA and ZOPS stimulation (Fig. 7D). These results demonstrate that mature neutrophils and macrophages differentiated from all the CGD iPSCs reproduce the expected pathognomonic CGD cellular phenotype.

Discussion

In this study we describe for the first time the establishment of *in vitro* models of three genetic forms of CGD (i.e., X^0-linked, AR47^0, and AR22^0) using patient-specific iPSCs obtained from human dermal fibroblasts. First, we performed both karyotyping and array-CGH assay to detect genomic aberrations in iPSC lines in order to discard aberrant clones. No abnormalities were found by karyotyping. However, two large telomeric duplications in an X^0-CGD clone were detected by array-CGH, which has a higher resolution than karyotype. In previous studies reporting the modeling of CGD from iPSCs, only karyotype was performed.[19–21] Then we checked that the mutations detected in the CGD patients were also found in iPSCs. The non-sense mutation 469C > T in exon 5 of *CYBB* leading to p.Arg157X in gp91^{phox}, which is a relatively common mutation as seen in Roos et al.[12] was successfully modelled. In addition, the *CYBA* mutation, a rare deletion c.295_301 delGTGCCCG found in exon 5, was reproduced in iPSCs and derived phagocytes.

We have to underline that the AR22^0-CGD form has not been modelled until now. The first human X-CGD form was modeled in 2011 by Zou et al. They produced neutrophils carrying a non-sense 458T > G mutation that is very close to our mutation.[20] One year later, two other X-linked mutations were modelled in macrophages using patient-specific iPS cells.[21] Our third iPS cell line is derived from a patient carrying the most frequent mutation (of more than 300 mutations listed[13]), c75_76delGT in *NCF1* leading to the p.Tyr26HisfsX26 defect in p47^{phox} and representing 95% of the AR47-CGD. The novelty is not only that we succeeded to model the AR22^0-CGD genetic form for the first time but also we managed to produce neutrophils and macrophages in parallel from the same pool of CD34$^+$ precursors using a simple, reproducible, and cheap protocol based on previous published work.[20,21,38]

Our choice of an efficient protocol for the production of both neutrophils and macrophages was guided by constraints of time, ease, differentiation, efficiency, and financial considerations. Hematopoietic differentiation was first described on mouse and human ESCs for the production of mature neutrophils and macrophages and then applied on iPSCs.[39–43] It was generally induced either through a first step of EB formation[20,21,39,41–45] or by a coculture of iPSCs with murine stromal OP9 cell lines.[18,19,25,46] The first step of our protocol was performed by inducing hematopoietic differentiation using iPSC/OP9 coculture system as previously described.[25] What is new is that we specified the production yield at each step of differentiation. Indeed, we succeeded in producing a high amount of CD34$^+$ progenitors (about $1–2.5 \times 10^6$ cells from 10×10^6 iPSCs, so several millions can be easily obtained by upscaling the culture conditions).

We have no comparison to data published by others, because quantitative data for the amount of precursors generated are rarely reported in the literature, especially from iPSC differentiation to obtain phagocytes. In addition, we characterized these CD34$^+$ precursors and found that they were mainly CD45$^-$ and CD43$^-$ (data not shown). We suppose that they are earlier hematopoietic progenitors than those produced by Choi et al.[18] Then we demonstrated for the first time that they conserved their hematopoietic potential toward myeloid lineage during freezing and thawing. This is an important point that simplifies the production of phagocytes. This first step was common for neutrophil and macrophage production and based on the simplification of Choi et al. differentiation protocol.[18] Contrary to Choi and collaborators, we did not isolate our cells by Percoll gradient, and we performed a CD34$^+$ cell sorting for neutrophil generation only.

We employed two different protocols to generate neutrophils and macrophages in parallel from the same pool of CD34-positive hematopoietic precursors. In comparison with other differentiation protocols that produced iPSC-derived neutrophils with only 30%–40% purity,[20,44] we improved the neutrophil purity to 50%–70%. We also quantified precisely the differentiation efficiency, a parameter not described before. Routinely from 5 million CD34$^+$ progenitors, about one million neutrophils could be easily generated. However, it seems to be easier to generate a large amount of neutrophils from ESCs compared with iPSCs.[39,40] A second point to underline is that our culture duration for mature neutrophil generation was 2–5 days shorter (25 days) than other protocols.[20,44] However, quantitative analysis of neutrophils produced showed that the yield of neutrophil differentiation compared to the input number of CD34$^+$ cells remains low. Attempt to expand the CD34$^+$ population was without success.

Macrophage generation from human iPSCs was easier than differentiation of neutrophils. In our protocol, cells were not CD34$^+$ sorted after the 10 days of hematopoietic differentiation. Short-term differentiation of coculture-derived cells into

multipotent myeloid progenitors as proposed by Choi et al. were sufficient to generate monocytes.[25] In our hands, a last step of adherence was necessary for terminal maturation and to improve the production yield and the purity.[21,45,47,48] Indeed, we succeeded to produce three billion pure (>90%) macrophages from ten million of iPSCs. The only article describing monocytes/macrophages' generation from CGD patient-specific iPSCs was published by Jiang et al.[21] and was based on EB differentiation as initially described by Karlsson et al. for ESCs.[42] Although they seemed to generate several million monocytes reproducibly, the purity and number of macrophages obtained were not clearly reported.[21] Two recent articles described an efficient but more expensive protocol for serum-free, feeder-free generation of monocytes/macrophages from iPSCs.[45,48]

Neutrophils and macrophages produced from control and the three CGD iPSC lines by our protocols were fully phenotypically and functionally characterized. CGD iPSC-derived phagocytic cells were analyzed by electron microscopy and appeared morphologically similar to human blood-derived neutrophils and macrophages. The presence of three populations of granules in control and CGD neutrophils was confirmed by cytochemical characterization (MPO-primary granules) and, for the first time, by demonstration of normal degranulation after fMLF stimulation (lactoferrin-secondary granules and MMP9-tertiary granules). Thus, these control and CGD iPSC-derived neutrophils are closer to blood-derived neutrophils than the HL60 or the PLB-985 cell lines, which do not possess secondary and tertiary granules.[49,50]

Concerning characterization of macrophages, we have not only analyzed the expression of the classical CD14, CD45, and CD11b antigen surface markers and costimulatory molecules CD40, CD80, and CD86, but we also determined the subtype of macrophages produced using a set of three cell markers: the mannose receptor (MR, CD206) expressed on professional phagocytic cells, major histocompatibility complex (MHC) class II cell surface receptor HLA-DR expressed on antigen presenting cells, and C-C chemokine receptor type 7 (CCR7, CD197) that was recently shown to be expressed on monocytes but only in the presence of the pro-inflammatory molecule PGE2.[51] The majority of macrophages produced were HLA-DR$^-$ CCR7$^-$, and MR$^+$, specific to the M2c subtype of macrophages, which are regulatory macrophages involved in immunosuppression and wound healing/tissue repair.[52] Human GM-CSF/interferon γ polarizes monocytes toward the M1 macrophage subtype, whereas treatment with M-CSF/IL-4 polarizes them to M2 macrophages. Therefore, it is not surprising to obtain M2 macrophages in our study after a step of terminal maturation performed in presence of M-CSF. Furthermore, we analyzed the cytokine release and confirmed previous results showing the production of IL-8 in resting macrophages.[21] In addition the production of IL-6, IL-8, IL-10, and TNFα were found in control and CGD iPS-derived macrophages stimulated by LPS.[21,42] Finally, phagocytosis experiments using particulate stimuli such as opsonized latex beads, *S. aureus* and zymosan showed that CGD iPSC-derived neutrophils and macrophages possessed a phagocytic potential comparable to those derived from WT iPSCs.

AR22^0-CGD iPSC-derived neutrophils and macrophages were generated for the first time in this study. We demonstrated that both subunits gp91^{phox} and p22^{phox} were absent in this cell line as well as in the X^0-CGD, while they were present in the WT and the AR47^0-CGD iPSCs. NBT test, fluorescent DHR, and the luminol-enhanced chemiluminescence assays showed that the phagocytic cells derived from the three CGD iPSC lines perfectly mimicked the oxidase-deficient phenotype as found in the original phagocytes from the CGD patients (data not shown). However, a residual activity was measured in the AR47^0-CGD iPSC-derived neutrophils when assessed by chemiluminescence, which is a very sensitive assay. Indeed, residual NADPH oxidase activity in the AR47^0-CGD patients' neutrophils are often described.[53] This proves that the AR47^0-CGD iPSC-derived neutrophils we generated are close to the original blood-derived AR47^0-CGD neutrophils.

Finally, we demonstrated that ROS deficiency does not have an effect on the kinetics and efficiency of hematopoietic differentiation by comparing the X^0-CGD and the WT iPSC lines in our conditions. Moreover, the genetic defect does not interfere with the potential of CGD iPSCs to generate mature neutrophils or macrophages, as previously shown by others.[19] Many studies are currently investigating the role of ROS during hematopoietic differentiation. Intracellular levels of ROS are strictly regulated in the bone marrow niche because thin balance is essential for maintenance of quiescence and self-renewal potential of hematopoietic stem cells as well as other functions such as survival/apoptosis, differentiation, and mobilization.[54,55] Further analysis of the specific role of ROS deficiency on the hematopoietic differentiation should be conducted by characterizing more precisely the different maturation steps of the X^0-CGD progenitors compared with the control cells and this, in both normoxia and hypoxia culture conditions.

In conclusion, the presented study aimed to establish an efficient, easy and reproducible protocol for generation of neutrophils and macrophages from iPSCs reprogrammed from patients carrying three genetic forms of CGD: X^0-linked, AR47^0-CGD, and for the first time, AR22^0-CGD. These *in vitro* cellular disease models represent promising tools that can be used for elucidating the pathophysiology of CGD and development of new therapeutic approaches for this disease. Furthermore, p22^{phox}, p47^{phox}, and gp91^{phox} expressed in several tissues and organs such as the brain, the kidney, and the cardiovascular tissue render these CGD cellular models relevant for the study of several pathologies connected with the absence of these subunits in these tissues.[56]

Acknowledgments

The work was supported by grants from Neurinox, European project, FP7—Theme 1 Health (2012–2015), Interreg France-Suisse (Programme de Coopération Territoriale Européenne, Fond Européen de Développement Régional (FEDER), 2013–2015). It was also supported by grants from Université Joseph Fourier Grenoble Alpes (AGIR program), the Medical School, and the Delegation for Clinical Research and Innovations (DRCI, Rementips project), Pôle Recherche, Centre Hospitalier Universitaire (CHU) Grenoble, Grenoble, France to J.B. and M.J.S; and the Köln Fortune Program (Medical Faculty, University of Koln, Germany) to T.S. We thank Charlotte Genestet, Sylvain Beaumel, Cécile Martel, and Michèle Mollin for their enthusiasm at work at the Centre Diagnostic et Recherche Sur la CGD (CDiReC), Rebecca Dieterich (Institute for Neurophysiology, Cologne, Germany) for technical

assistance, Dr Franck Pellestor (CHU Montpellier, Laboratoire de Génétique Chromosomique) for the gift of the karyotyping protocol (personal communication), and Sébastien Bailly for the statistical analysis. Special thanks are extended to David Laurin for the irradiation of MEFs.

Author Disclosure Statement

No competing financial interests exist.

References

1. Takahashi K, Yamanaka S. Induction of pluripotent stem cells from mouse embryonic and adult fibroblast cultures by defined factors. Cell. 2006;126:663–676.
2. Takahashi K, Tanabe K, Ohnuki M, et al. Induction of pluripotent stem cells from adult human fibroblasts by defined factors. Cell. 2007;131:861–872.
3. Yu J, Vodyanik MA, Smuga-Otto K, et al. Induced pluripotent stem cell lines derived from human somatic cells. Science. 2007;318:1917–1920.
4. Park I-H, Arora N, Huo H, et al. Disease-specific induced pluripotent stem cells. Cell. 2008;134:877–886.
5. González F, Boué S, Izpisúa Belmonte JC. Methods for making induced pluripotent stem cells: reprogramming à la carte. Nat Rev Genet. 2011;12:231–242.
6. Fatima A, Kaifeng S, Dittmann S, et al. The disease-specific phenotype in cardiomyocytes derived from induced pluripotent stem cells of two long QT syndrome type 3 patients. PloS One. 2013;8:e83005.
7. Raya A, Rodríguez-Pizà I, Guenechea G, et al. Disease-corrected haematopoietic progenitors from Fanconi anaemia induced pluripotent stem cells. Nature. 2009;460:53–59.
8. Ross CA, Akimov SS. Human-induced pluripotent stem cells: potential for neurodegenerative diseases. Hum Mol Genet. 2014;23:R17–R26.
9. Ordonez MP, Goldstein LSB. Using human-induced pluripotent stem cells to model monogenic metabolic disorders of the liver. Semin Liver Dis. 2012;32:298–306.
10. Robinton DA, Daley GQ. The promise of induced pluripotent stem cells in research and therapy. Nature. 2012;481:295–305.
11. Van den Berg JM, van Koppen E, Ahlin A, et al. Chronic granulomatous disease: the European experience. PloS One. 2009;4:e5234.
12. Roos D, Kuhns DB, Maddalena A, et al. Hematologically important mutations: X-linked chronic granulomatous disease (third update). Blood Cells Mol Dis. 2010;45:246–265.
13. Roos D, Kuhns DB, Maddalena A, et al. Hematologically important mutations: the autosomal recessive forms of chronic granulomatous disease (second update). Blood Cells Mol Dis. 2010;44:291–299.
14. Matute JD, Arias AA, Wright NAM, et al. A new genetic subgroup of chronic granulomatous disease with autosomal recessive mutations in p40 phox and selective defects in neutrophil NADPH oxidase activity. Blood. 2009;114:3309–3315.
15. Seger RA, Gungor T, Belohradsky BH, et al. Treatment of chronic granulomatous disease with myeloablative conditioning and an unmodified hemopoietic allograft: a survey of the European experience, 1985–2000. Blood. 2002;100:4344–4350.
16. Kang EM, Malech HL. Gene therapy for chronic granulomatous disease. Methods Enzymol. 2012;507:125–154.
17. Zhen L, King AA, Xiao Y, et al. Gene targeting of X chromosome-linked chronic granulomatous disease locus in a human myeloid leukemia cell line and rescue by expression of recombinant gp91phox. Proc Natl Acad Sci U S A. 1993;90:9832–9836.
18. Choi K-D, Vodyanik MA, Slukvin II. Generation of mature human myelomonocytic cells through expansion and differentiation of pluripotent stem cell–derived lin–CD34+ CD43+CD45+ progenitors. J Clin Invest. 2009;119:2818–2829.
19. Mukherjee S, Santilli G, Blundell MP, et al. Generation of functional neutrophils from a mouse model of X-linked chronic granulomatous disorder using induced pluripotent stem cells. PLoS ONE. 2011;6:e17565.
20. Zou J, Sweeney CL, Chou B-K, et al. Oxidase-deficient neutrophils from X-linked chronic granulomatous disease iPS cells: functional correction by zinc finger nuclease–mediated safe harbor targeting. Blood. 2011;117:5561–5572.
21. Jiang Y, Cowley SA, Siler U, et al. Derivation and functional analysis of patient-specific induced pluripotent stem cells as an in vitro model of chronic granulomatous disease. Stem Cells. 2012;30:599–611.
22. Okita K, Matsumura Y, Sato Y, et al. A more efficient method to generate integration-free human iPS cells. Nat Methods. 2011;8:409–412.
23. Yu J, Chau KF, Vodyanik MA, Jiang J, Jiang Y. Efficient feeder-free episomal reprogramming with small molecules. PloS One. 2011;6:e17557.
24. Shao K, Koch C, Gupta MK, et al. Induced pluripotent mesenchymal stromal cell clones retain donor-derived differences in DNA methylation profiles. Mol Ther. 2013;21:240–250.
25. Choi K-D, Vodyanik M, Slukvin II. Hematopoietic differentiation and production of mature myeloid cells from human pluripotent stem cells. Nat Protoc. 2011;6:296–313.
26. Carrichon L, Picciocchi A, Debeurme F, et al. Characterization of superoxide overproduction by the D-Loop(Nox4)-Nox2 cytochrome b(558) in phagocytes-Differential sensitivity to calcium and phosphorylation events. Biochim Biophys Acta. 2011;1808:78–90.
27. Burritt JB, Busse SC, Gizachew D, et al. Antibody imprint of a membrane protein surface. Phagocyte flavocytochrome b. J Biol Chem. 1998;273:24847–24852.
28. Hattori K. An improved method of peroxidase reaction combined with Giemsa's stain for blood cells. J Lab Clin Med. 1958;51:829–834.
29. Preynat-Seauve O, Suter DM, Tirefort D, et al. Development of human nervous tissue upon differentiation of embryonic stem cells in three-dimensional culture. Stem Cells. 2009;27:509–520.
30. Trocmé C, Gaudin P, Berthier S, et al. Human B lymphocytes synthesize the 92-kDa gelatinase, matrix metalloproteinase-9. J Biol Chem. 1998;273:20677–20684.
31. Nuutila J, Lilius E-M. Flow cytometric quantitative determination of ingestion by phagocytes needs the distinguishing of overlapping populations of binding and ingesting cells. Cytometry. 2005;65:93–102.
32. Defendi F, Decleva E, Martel C, Dri P, Stasia MJ. A novel point mutation in the CYBB gene promoter leading to a rare X minus chronic granulomatous disease variant - impact on the microbicidal activity of neutrophils. Biochim Biophys Acta. 2009;1792:201–210.
33. Picciocchi A, Debeurme F, Beaumel S, et al. Role of putative second transmembrane region of Nox2 protein in the structural stability and electron transfer of the phagocytic NADPH oxidase. J Biol Chem. 2011;286:28357–28369.

34. Bakri FG, Martel C, Khuri-Bulos N, et al. First report of clinical, functional, and molecular investigation of chronic granulomatous disease in nine Jordanian families. J Clin Immunol. 2009;29:215–230.
35. Stasia MJ, Mollin M, Martel C, et al. Functional and genetic characterization of two extremely rare cases of Williams-Beuren syndrome associated with chronic granulomatous disease. Eur J Hum Genet. 2013;21:1079–1084.
36. Coutton C, Dieterich K, Satre V, et al. Array-CGH in children with mild intellectual disability: a population-based study. Eur J Pediatr. 2014. [Epub ahead of print]; DOI: 10.1007/s00431-014-2367-6.
37. Vodyanik MA, Bork JA, Thomson JA, Slukvin II. Human embryonic stem cell-derived CD34+ cells: efficient production in the coculture with OP9 stromal cells and analysis of lymphohematopoietic potential. Blood. 2005;105:617–626.
38. Choi K-D, Yu J, Smuga-Otto K, et al. Hematopoietic and endothelial differentiation of human induced pluripotent stem cells. Stem Cells. 2009;27:559–567.
39. Lieber JG, Webb S, Suratt BT, et al. The in vitro production and characterization of neutrophils from embryonic stem cells. Blood. 2004;103:852–859.
40. Saeki K, Saeki K, Nakahara M, et al. A feeder-free and efficient production of functional neutrophils from human embryonic stem cells. Stem Cells. 2009;27:59–67.
41. Yokoyama Y, Suzuki T, Sakata-Yanagimoto M, et al. Derivation of functional mature neutrophils from human embryonic stem cells. Blood. 2009;113:6584–6592.
42. Karlsson KR, Cowley S, Martinez FO, et al. Homogeneous monocytes and macrophages from human embryonic stem cells following coculture-free differentiation in M-CSF and IL-3. Exp Hematol. 2008;36:1167–1175.
43. Subramanian A, Guo B, Marsden MD, et al. Macrophage differentiation from embryoid bodies derived from human embryonic stem cells. Stem Cells. 2009;4:29–45.
44. Morishima T, Watanabe K, Niwa A, et al. Neutrophil differentiation from human-induced pluripotent stem cells. J Cell Physiol. 2011;226:1283–1291.
45. Wilgenburg B van, Browne C, Vowles J, Cowley SA. Efficient, long term production of monocyte-derived macrophages from human pluripotent stem cells under partly-defined and fully-defined conditions. PLoS ONE. 2013;8:e71098.
46. Anderson JS, Bandi S, Kaufman DS, Akkina R. Derivation of normal macrophages from human embryonic stem (hES) cells for applications in HIV gene therapy. Retrovirology. 2006;3:24.
47. Senju S, Haruta M, Matsumura K, et al. Generation of dendritic cells and macrophages from human induced pluripotent stem cells aiming at cell therapy. Gene Ther. 2011; 18:874–883.
48. Yanagimachi MD, Niwa A, Tanaka T, et al. Robust and highly-efficient differentiation of functional monocytic cells from human pluripotent stem cells under serum- and feeder cell-free conditions. PloS One. 2013;8:e59243.
49. Collins SJ, Gallo RC, Gallagher RE. Continuous growth and differentiation of human myeloid leukaemic cells in suspension culture. Nature. 1977;270:347–349.
50. Tucker KA, Lilly MB, Heck L Jr, Rado TA. Characterization of a new human diploid myeloid leukemia cell line (PLB-985) with granulocytic and monocytic differentiating capacity. Blood. 1987;70:372–378.
51. Côté SC, Pasvanis S, Bounou S, Dumais N. CCR7-specific migration to CCL19 and CCL21 is induced by PGE2 stimulation in human monocytes: Involvement of EP2/EP4 receptors activation. Mol Immunol. 2009;46:2682–2693.
52. Mantovani A, Sica A, Sozzani S, et al. The chemokine system in diverse forms of macrophage activation and polarization. Trends Immunol. 2004;25:677–686.
53. Köker MY, Camcıoğlu Y, van Leeuwen K, et al. Clinical, functional, and genetic characterization of chronic granulomatous disease in 89 Turkish patients. J Allergy Clin Immunol. 2013;132:1156–1163.
54. Sardina JL, López-Ruano G, Sánchez-Sánchez B, Llanillo M, Hernández-Hernández A. Reactive oxygen species: are they important for haematopoiesis? Crit Rev Oncol Hematol. 2012;81:257–274.
55. Urao N, Ushio-Fukai M. Redox regulation of stem/progenitor cells and bone marrow niche. Free Radic Biol Med. 2013;54:26–39.
56. Bedard K, Krause K-H. The NOX family of ROS-generating NADPH oxidases: physiology and pathophysiology. Physiol Rev. 2007;87:245–313.

Address correspondence to:
Julie Brault, PharmD
Techniques de l' Ingénierie Médicale
et de la Complexité-Informatique
Mathématiques et Applications
Grenoble (TIMC-IMAG)
Université Grenoble Alpes
UMR CNRS 5525
Grenoble F-38000
France

E-mail: jbrault@chu-grenoble.fr

Marie José Stasia, PharmD, PhD
Techniques de l' Ingénierie Médicale
et de la Complexité-Informatique
Mathématiques et Applications
Grenoble (TIMC-IMAG)
Université Grenoble Alpes
UMR CNRS 5525
Grenoble F-3800
France

E-mail: mjstasia@chu-grenoble.fr

Abbreviations Used

αFP = anti-α-fetoprotein
αSMA = anti-α-smooth muscle actin
AF647 = AlexaFluor647
array-CGH = array-comparative genomic hybridization
CFU = colony forming units
CGD = chronic granulomatous disease
CNV = copy number variation
DHR = dihydrorhodamine-1,2,3
DMEM = Dulbecco's modified Eagle medium
DMSO = dimethylsulfoxyde
EBs = embryoid bodies
ESC = embryonic stem cell
FACS = fluorescence-activated cell sorting buffer
FBS = fetal bovine serum

Abbreviations Used (Cont.)

FITC = fluorescein isothiocyanate fluorescein
fMLF = f-Met-Leu-Phe
GM-CSF = granulocytemacrophage colony-stimulating factor
hDFs = human dermal fibroblasts
HLA-DR = human leukocyte antigen-DR
HRPO = horseradish peroxidase
IgG = immunoglobin G
IMDM = Iscove's modified Dulbecco's medium
iPSCs = induced pluripotent stem cells
KOSR = KnockOut™ Sermus Replacement
LPS = lipopolysaccharides
MACS = magnetic cell sorting
M-CSF = macrophage colony-stimulating factor
MEF = mouse embryonic fibroblast
MEM = α-minimum essential medium
MGG = May-Grunwald-Giemsa
MMP9 = matrix-metalloprotease 9
MPO = myeloperoxidase
MR = mannose receptor
MTG = monothioglycerol
NADPH = nicotinamide-adenine-dinucleotidephosphate
NBT = nitro blue tetrazolium
NEAA = nonessential amino acids
PBS = phosphate-buffered saline
PE = anti-CD31-coupled phycoerythrin
pHEMA = poly-hydroxy-ethyl-methacrylatecoated
ROS = reactive oxygen species
S = Supernatants
SSEA-4 = anti-stage-specific embryonic antigen-4